

NEXT STATE PREDICTION GIVES RISE TO ENTANGLED, YET COMPOSITIONAL REPRESENTATIONS OF OBJECTS

Tankred Saanum^{1,†} Luca M. Schulze Buschoff² Peter Dayan^{*,1,3} Eric Schulz^{*,2}

[†]tankred.saanum@tuebingen.mpg.de

ABSTRACT

Compositional representations are thought to enable humans to generalize across combinatorially vast state spaces. Models with learnable object slots, which encode information about objects in separate latent codes, have shown promise for this type of generalization but rely on strong architectural priors. Models with distributed representations, on the other hand, use overlapping, potentially entangled neural codes, and their ability to support compositional generalization remains underexplored. In this paper we examine whether distributed models can develop linearly separable representations of objects, like slotted models, through unsupervised training on videos of object interactions. We show that, surprisingly, models with distributed representations often match or outperform models with object slots in downstream prediction tasks. Furthermore, we find that linearly separable object representations can emerge without object-centric priors, with auxiliary objectives like next-state prediction playing a key role. Finally, we observe that distributed models’ object representations are never fully disentangled, even if they are linearly separable: Multiple objects can be encoded through partially overlapping neural populations while still being highly separable with a linear classifier. We hypothesize that maintaining partially shared codes enables distributed models to better compress object dynamics, potentially enhancing generalization.

1 INTRODUCTION

Humans naturally decompose scenes, events and processes in terms of the objects that feature in them (Tenenbaum et al., 2011; Lake et al., 2017). These object-centric construals have been argued to explain humans’ ability to reason and generalize successfully (Goodman et al., 2008; Lake et al., 2015; Schulze Buschoff et al., 2023). It has therefore long been a chief aim in machine learning research to design models and agents that learn to represent the world compositionally, e.g. in terms of the building blocks that compose it. In computer vision, models with *object slots* learn to encode scenes into a latent, compositional code, where each object in the scene is modelled by a distinct part of the latent space. This strong architectural assumption allows the models to learn representations that improve compositional generalization (Brady et al., 2023; Wiedemer et al., 2023) and reasoning about objects (Wu et al., 2022).

Slotted representations are often contrasted with distributed representations. Models with distributed representations encode information about a scene, and potentially the objects that compose it, in overlapping populations of neurons. Can models with distributed representations learn to encode objects in a compositional way without supervision? And can distributed coding schemes offer advantages over *purely* object-centric coding schemes?

By compressing properties of multiple objects in a shared code, models with distributed representations could potentially gain richer representations where scene similarities are more abundant (Smola

¹Max Planck Institute for Biological Cybernetics, Tübingen, Germany

²Institute for Human-Centered AI, Helmholtz Computational Health Center, Munich, Germany

³University of Tübingen

*Equal advising.

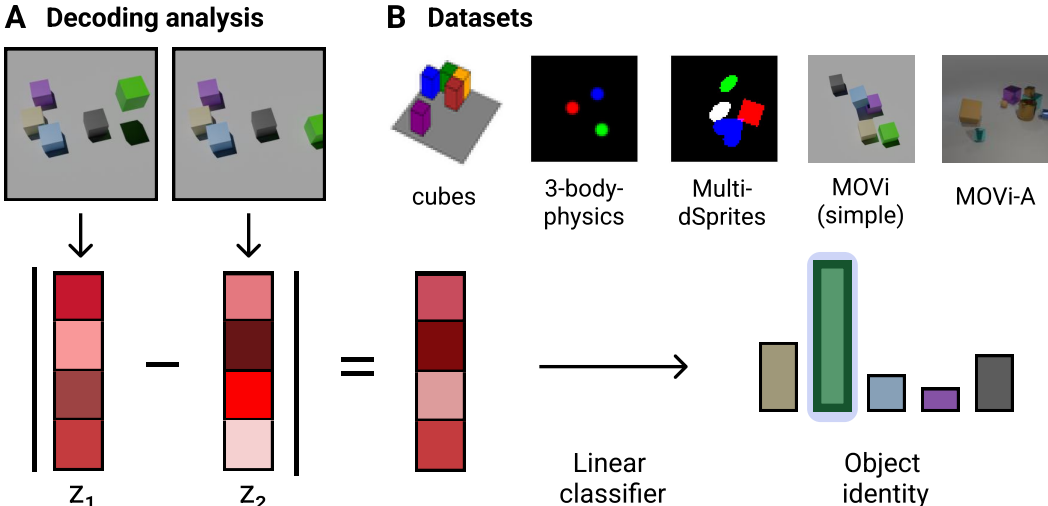


Figure 1: Overview of the decoding analysis and datasets. **A**: We propose a simple test for assessing compositional object representations. After unsupervised pre-training on object videos, we evaluate the linear separability of models’ latent object representations. This is done by training a linear classifier on the absolute differences of two successive encoded frames where only one object changes. **B**: We evaluate the models on five datasets of dynamically interacting objects, ranging from simple depictions of blocks and sprites to realistic simulations of 3D objects.

& Schölkopf, 1998; Lucas et al., 2015; Demircan et al., 2023; Garvert et al., 2023). For instance, if two objects are represented similarly, the model could use what it knows about the dynamics of one object to generalize about the dynamics of the other object. This could in turn facilitate learning, potentially at the loss of fully separable object representations.

In our study, we offer experimental evidence that **models with distributed representations can learn compositional construals of objects** in an unsupervised manner, when trained on sufficiently large datasets. Across 5 datasets that consist of dynamically interacting objects we see that models with distributed representations either match or outperform their slot-based counterparts in the tasks they were trained to perform (image reconstruction or dynamics prediction). Next, we define a simple metric inspired by Higgins et al. (2016) that quantifies how accurately object identities can be linearly decoded from a model’s latent representations (see Figure 1). We see that as training data size increases, the models with distributed representations develop gradually more disentangled representations of objects. However, while object representations become separable, their properties remain encoded through *partially* overlapping populations of neurons, potentially allowing for richer generalization. Investigating the effect of training objective and loss function on the separability metric, we find that next-state prediction is a crucial component for the development of separable object representations for models without object slots.

While we see object disentanglement emerge without any supervision or regularization, this disentanglement is not absolute. Distributed models represent object properties in partially shared latent spaces. We speculate that this can facilitate generalization: When comparing models’ representations of object dynamics, we see clear clustering based on object identity (indicating separable object representations), but also clustering based on what type of transformation was applied to the object. This means that transformations such as object rotations, object scaling or object movements are represented more similarly, independently of which object they are applied to. Such compositional codes for group transformations of objects are made possible by the fact that all objects share a common latent space, instead of occupying separate ones, suggesting that there are benefits to distributed coding schemes.

2 RELATED WORK

Object-centric representations have been argued to improve the sample efficiency and generalization ability of vision and dynamics models in compositional domains (Elsayed et al., 2022; Kipf et al., 2019; Wiedemer et al., 2023; Wu et al., 2022; Locatello et al., 2020b). Object-centric representations, given an appropriate model architecture, can also be learned in an unsupervised manner (Kipf et al., 2019; Locatello et al., 2020b; Brady et al., 2023) and on real-world datasets (Seitzer et al., 2022). Previous studies have highlighted the importance of architectural features, like object-slots (Greff et al., 2020; 2019; Dittadi et al., 2021), as well as data properties, like having access to temporal information (Zadaianchuk et al., 2024).

There is a considerable overlap in the literature on object-centric and disentangled representations. A disentangled representation is one “which separates the factors of variation, explicitly representing the important attributes of the data” (Bengio et al., 2013; Locatello et al., 2020a; Higgins et al., 2016; 2018). In a disentangled representation, a change in a single ground truth factor should lead to a change in a single factor in the learned representation (Locatello et al., 2019; Ridgeway & Mozer, 2018; Kim & Mnih, 2018). Information bottlenecks methods like β -VAEs have also been shown to be able to disentangle object features (Burgess et al., 2018; Higgins et al., 2017).

In recent work, Brady et al. (2023) put forward a measure of representational object-centricity that measures “if there exists an invertible function between each ground-truth slot and exactly one inferred latent slot”. We work with a related metric suitable for generic model classes (e.g. without image decoders) that instead measures the degree to which changes to individual objects can be predicted from changes in a model’s latent representations.

3 METHODS

3.1 MODELS

We focus on models that learn representations of scenes in an unsupervised manner, e.g. without information about object identities provided as labels or masks. Unsupervised training regimes, such as auto-encoding (Kingma, 2013), denoising (He et al., 2022) and contrastive objectives (Chen et al., 2020) have shown promise as representation learning tools in many domains, ranging from image and language understanding (Radford et al., 2021) to reinforcement learning (Schwarzer et al., 2020; Gelada et al., 2019; Saanum et al., 2024). In this paper we investigate two classes of such training objectives: *i*) Reconstruction-based or auto-encoding objectives, where the goal is to encode and reconstruct images of scenes of objects. And *ii*), contrastive objectives, where the goal is to maximize embedding similarities of positive pairs and minimize similarities of negative pairs. Accordingly, the models rely on an image encoder, a Convolutional Neural Net (CNN) in our case, to map images of objects to latent representations. For auto-encoding models we additionally equip the model with a CNN decoder that maps the latent representation back to pixel-space.

$$z_t = e_\theta(x_t) \tag{1}$$

$$\tilde{x}_t = g_\theta(z_t) \tag{2}$$

Here z_t is the model’s representation, and e_θ and g_θ are the CNN encoder and decoder. x_t and \tilde{x}_t are the image and reconstruction, respectively. We subscript image and representation variables with the time-point t since our data are dynamic. Having access to this temporal information about the data, we also consider models that use future-state prediction as an auxiliary objective for representation learning. Observing how objects interact dynamically can provide the models with useful cues about object identities, and could facilitate learning systematic representations of objects (Zadaianchuk et al., 2024). When modelling the dynamics of the object data, we equip the model with a latent dynamics module that predicts the model’s representation at the next time point $t + 1$, given the current representation, and an action a_t , if the dynamics data is accompanied by actions.

$$\tilde{z}_{t+1} = d_\theta(z_t, a_t) \tag{3}$$

Here d_θ denotes the dynamics module, which is a Multi-Layer Perceptron (MLP) in the case that the dynamics are Markovian, e.g. fully predictable from the information provided in the current observation x_t (and potentially action a_t). In non-Markovian settings we use a causal Transformer that integrates information across representations of past observations ($z_{t-n}, \dots, z_{t-1}, z_t$) to predict the dynamics. See Appendix B for details on the model architecture and hyperparameters.

For the auto-encoding models, we train the encoder and decoder to reconstruct the *current* frame from the current representation in the static setting, and the *next* frame from the predicted *next* latent representation in the dynamic setting. Here, we additionally train the dynamics model to minimize the distance between the predicted and actual representation of the next frame. This leaves us with the following loss functions:

$$\mathcal{L}_{\text{AE-static}} = \|x_t - g_\theta(z_t)\|_2^2 \quad (4)$$

$$\mathcal{L}_{\text{AE-dynamic}} = \|x_{t+1} - g_\theta(\tilde{z}_{t+1})\|_2^2 + \|z_{t+1} - d_\theta(z_t, a_t)\|_2^2 \quad (5)$$

We refer to these models as the *auto-encoder* and *sequential auto-encoder*, respectively.

For the contrastive models, we consider both a static and dynamic training scheme as well. In the static case, we present the model with a frame x_t as well as a randomly augmented view of the same frame $h(x_t)$ (Laskin et al., 2020; Grill et al., 2020). The model is then trained to minimize the embedding distance between the original and augmented view of the image, while maximizing the embedding distance between the original image and its representations of augmented views of other frames x^- in the batch, up to a margin λ . In the dynamic setting we train the contrastive model as follows: Given an initial latent representation (and potentially action), we train the encoder and dynamics model to produce a prediction that is as close as possible to the encoded representation of the next frame z_{t+1} , and that is maximally far away from encoded representations of other frames z^- , up to a margin λ . The loss functions take the following form:

$$\mathcal{L}_{\text{contrastive-static}} = \|z_t - e_\theta(h(x_t))\|_2^2 + \max(0, \lambda - \|e_\theta(h(x^-)) - z_t\|_2^2) \quad (6)$$

$$\mathcal{L}_{\text{contrastive-dynamic}} = \|z_{t+1} - d_\theta(z_t, a_t)\|_2^2 + \max(0, \lambda - \|z^- - d_\theta(z_t, a_t)\|_2^2) \quad (7)$$

We refer to the static contrastive model as *CRL*, for Contrastive Representation Learner, and the dynamic contrastive model as *CWM*, for Contrastive World Model.

3.1.1 SLOTTED MODELS

We compare the auto-encoding models and CWM to baselines which attempt to learn slotted representations. As a baseline to the auto-encoding models, we implement Slot Attention (Locatello et al., 2020b), an auto-encoder that reconstructs images as an additive composition of multiple object slots. The slots compete to represent the objects in the scene using an iterative attention mechanism, and the full model is trained with a simple auto-encoding objective as in equation 5.

The contrastive dynamics model is compared to a *structured* variant, the Contrastive Structured World Model (CSWM) (Kipf et al., 2019), that decomposes the scene into distinct object slots, and uses a graph neural network to predict how these object slots evolve over time. In non-Markovian settings, we replace the graph neural network with a Transformer encoder that applies spatio-temporal attention over a sequence of past object-slot representations, akin to the Slotformer architecture (Wu et al., 2022). Here too, the loss function exactly matches the one used to train the contrastive dynamics model with distributed representations.

3.2 ASSESSING OBJECT REPRESENTATIONS

How can we quantify the degree to which a non-slotted model has learned systematic object representations? While many metrics are possible, we propose one which is both simple and has connections to other metrics proposed to quantify representation disentanglement. If a representation of an object o_i is disentangled from representations of other objects o' , then a change to o_i should only change one subspace of the models' latent representation z . Additionally, this subspace should

not be affected by changes to any of the other objects o' . In other words, each object is represented across completely non-overlapping populations of neurons. Complete disentanglement is a tall order for models without the structural properties of slotted models. To get a continuous relaxation of this absolute object disentanglement metric we ask a related question of the models' latent spaces: Given a set of changes to individual objects in a scene, how accurately can a linear classifier predict which object was changed from the resulting absolute difference in the model's latent representations? The accuracy of this linear classifier on an evaluation set is our proposed metric. This metric is in fact a variation of the disentanglement metric proposed in [Higgins et al. \(2016\)](#), but applied to objects rather than ground truth generative features. Even if a model attains a perfect score on this metric, it does not necessarily mean that it represent objects in perfectly disjoint, non-overlapping populations of neurons. To illustrate, if a change to object o_i always changes latent z^1 marginally and latent z^2 greatly, and a change to object o_j changes z^1 greatly and z^2 marginally, a linear classifier can reliably separate the two objects in terms of the change in z , despite them having entangled representations. In other words, it is possible to use overlapping neural codes to represent objects, while still having object representations that are linearly separable. We investigate this further in [Section 5](#).

In practice, we implement our metric by constructing datasets consisting of pairs of images (x_t^i, x_{t+1}^i) from the data domain on which a model was trained. The only difference between these two images is that a single object has changed from time t to $t + 1$. For each such pair we associate it with a label y^i , a categorical variable indicating *which* object was altered from t to $t + 1$. We then extract a model's representation of each frame in the pair (after it has been trained), and compute the vector of absolute differences between these two representations:

$$|\Delta^i| = |e_\theta(x_t^i) - e_\theta(x_{t+1}^i)| \quad (8)$$

From the set of ensuing absolute difference vectors $\mathcal{X} = (|\Delta^1|, \dots, |\Delta^n|)$ we train a linear classifier to predict the corresponding object labels $\mathcal{Y} = (y^1, \dots, y^n)$ while minimizing the L_1 norm of the learned coefficients, as recommended by [Higgins et al. \(2016\)](#). We report the accuracy on a left out subset of $(\mathcal{X}, \mathcal{Y})$ that the classifier was not trained on.

4 EXPERIMENTS

We trained the two classes of distributed models, as well as their object-centric counterparts, on five datasets of dynamically interacting objects. Two of these datasets, `cubes` and `3-body physics`, were introduced in [Kipf et al. \(2019\)](#) to showcase how object-centric representations facilitate learning of object dynamics. Extending the evaluation, we created our own dataset of object interactions based on the dSprites environment ([Matthey et al., 2017](#)). This dataset consisted of four sprites with different shapes and colors traversing latent generative factors, such as (x, y) -coordinates, scale and orientation, on a random walk. Lastly, we trained our models on two more complex Multi-Object Video (MOVi) datasets generated using the Kubric simulator ([Greff et al., 2022](#)), a 3D physics engine for simulating realistic object interactions. We generated one dataset consisting of 14,000 videos with a constant set of five cubes with fixed physical properties that interacted (initial object conditions such as directional velocities and position were randomized for each video). We refer to this dataset as `MOVi (simple)`, due to the constant object properties. Additionally we trained models on the `MOVi-A` dataset, consisting of almost 10,000 videos where the number of objects, their shapes and physical properties, such as mass and friction, are not fixed and vary across videos. The `cubes` and `Multi-dSprites` datasets had action variables that accompanied the videos, and were predictive of the way the objects would change from one frame to another. The other datasets were action-free. All models were trained for 100 epochs with five random seeds on the `cubes`, `3-body physics` and `multi-dSprites` datasets, and for 125 epochs with three random seeds on the `MOVi` datasets. Furthermore, to assess the effect of dataset size on our evaluation metrics, we split each dataset up in different sizes.

We evaluated the slotted CSWM and distributed CWM models' prediction abilities by measuring the accuracy with which they could predict novel object trajectories of length n from an unseen evaluation set in an open loop manner. Prediction accuracy was estimated as the percentage of test trajectories where the predicted latent state \tilde{z}_{t+n} at the end of the trajectory was closest in terms of Euclidean distance to the model's representation of the last frame in the trajectory z_{t+n} out of 1000

evaluation trajectories. For the `cubes`, `3-body physics` and `Multi-dSprites` datasets, we conducted the evaluations with a trajectory length of $n = 10$, and a trajectory length of $n = 3$ in the more complex `MOVi` datasets.

To assess object-separability we created evaluation videos for all five datasets. In these evaluation sets only single objects from the respective object domain were changed while all other objects in the scene remained fixed. After training models on each of the datasets, we assessed how well one could linearly classify which object had moved using the protocol described in Section 3.2.

4.1 OBJECT SLOTS ARE NOT NECESSARY FOR LEARNING OBJECT DYNAMICS

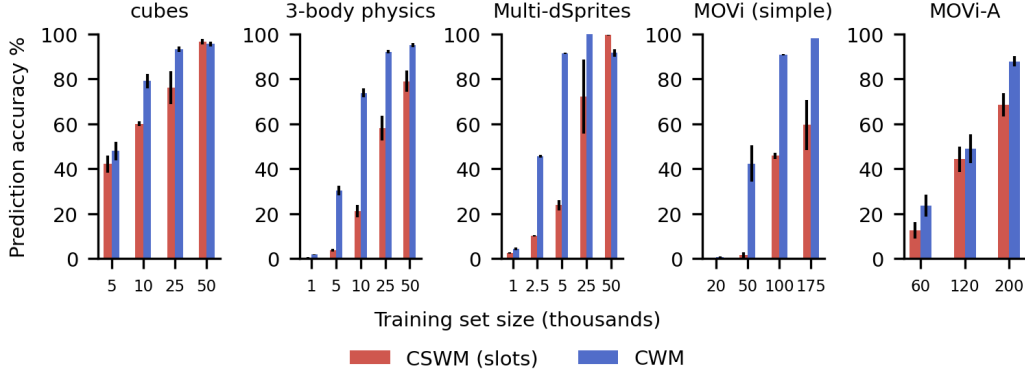


Figure 2: Prediction accuracies for slotted and non-slotted contrastive dynamics models. In all five datasets we see that the CWM is not only competitive, but sometimes outperforms the CSWM when it comes to predicting object dynamics. Scores are averaged over five seeds, with error bars depicting the standard error of the mean.

Evaluating the prediction accuracy of the CSWM and CWM, we observe that object-slots are not necessary for accurately predicting object dynamics. In fact, the CWM models often outperformed their slotted counterparts (see Figure 2). As expected, we see test accuracy generally increase with training set size. This suggests that compositional generalization about objects, the ability to generalize about properties of objects in novel constellations and combinations, does not require explicit object-centric priors as provided by slotted architectures.

4.2 PREDICTING OBJECT DYNAMICS IMPROVES OBJECT SEPARABILITY

If models without object-slots can successfully generalize about object dynamics in combinatorially novel scenarios, is this because they too develop separable and compositional representations of objects? We evaluated the degree to which CWM’s representations of objects were linearly separable. Here we observe that representations of objects get more and more separable with a linear decoder as the models are provided with more training examples. In simpler domains like the `cubes` and `3-body physics`, the models attain scores close to a 100% in the largest data setting (see Figure 3). In the more challenging domains like `Multi-dSprites` and the `MOVi` environments, where multiple objects are moving and interacting simultaneously, the decodability is lower, but substantially larger than chance at around 70%. For comparison, evaluating randomly initialized networks with the same metric only gives slightly better than chance object decodability scores, meaning that default representations for these models are strongly entangled (see Appendix C). Moreover, we see the same trend where larger training set sizes translate to better decodability. This suggests that, even for complex datasets with multiple interacting, realistically rendered objects, systematic and separable representations of objects can potentially emerge with scale.

To assess the importance of next-state prediction, we evaluate the object-separability of the CRL’s representations. Surprisingly, the CRL attains separability scores that are close to chance, suggesting that training on dynamic object data offers valuable information for learning composable representations in the contrastive setting.

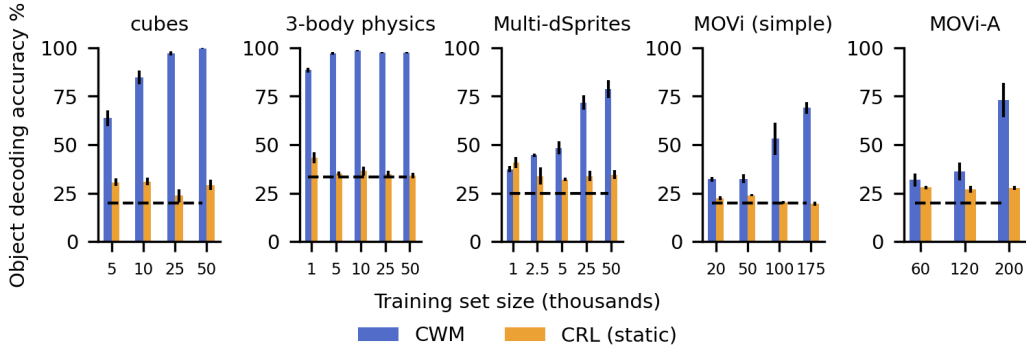


Figure 3: Object decoding accuracy as a function of training set size, for contrastive models. CWM representations of objects become more linearly separable with dataset size, despite no architectural components that encourage the formation of object-centric representations. However, contrastive learning without next step prediction (CRL) does not give rise to object-centric representations, suggesting an important role for information provided by dynamic data. Scores are averaged over five seeds (three seeds in the MOVi domains), with error bars depicting standard error of the mean.

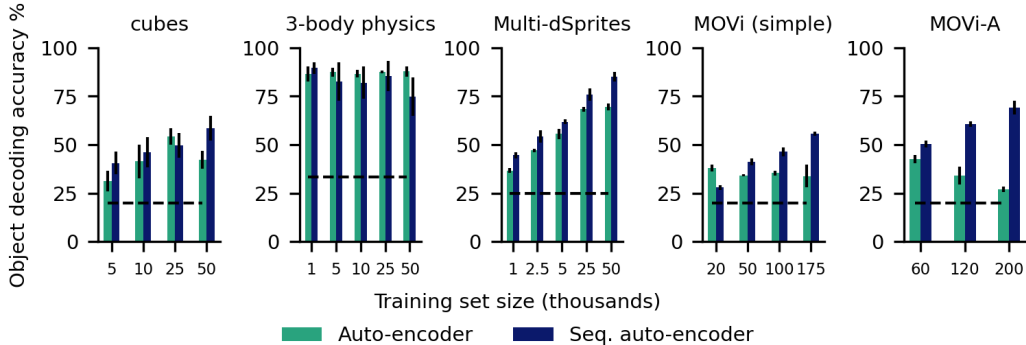


Figure 4: Object decoding accuracy as a function of training set size, for auto-encoding models. The dynamic training scheme yields a monotonic increase in object separability with training set size in four out of five datasets. Scores are averaged over five seeds (three seeds in MOVi domains), with error bars depicting standard error of the mean.

Do these trends hold for models with non-contrastive learning objectives? We evaluated the static and sequential variants of the auto-encoding models. First, we observe a significantly stronger tendency for the *sequential* auto-encoder to develop separable object representations (see Figure 4). This also suggests that providing the models with information about object dynamics in the form of a training signal can facilitate the development of composable object representations. In fact, it is only in the *Multi-dSprites* domain that the static autoencoder shows a monotonic increase in object separability with training set size. Comparing auto-encoding objectives to the contrastive objective, we see that object separability was generally lower for auto-encoding models in the *cubes* and *3-body physics* datasets.

Next we assessed the reconstruction quality of the static and sequential auto-encoder, and compared them to Slot Attention. We used the LPIPS (Zhang et al., 2018) perceptual similarity metric to quantify reconstruction fidelity on novel object configurations in the *MOVi-A* and *MOVi (simple)* datasets. While we see that Slot Attention has a small edge on the distributed models in terms of fidelity, both the static and sequential auto-encoder approach Slot Attention with more data (see Figure 5). Lastly, the auto-encoder performs better than the sequential auto-encoder on the test set, despite attaining substantially lower object separability scores in the MOVi domain.

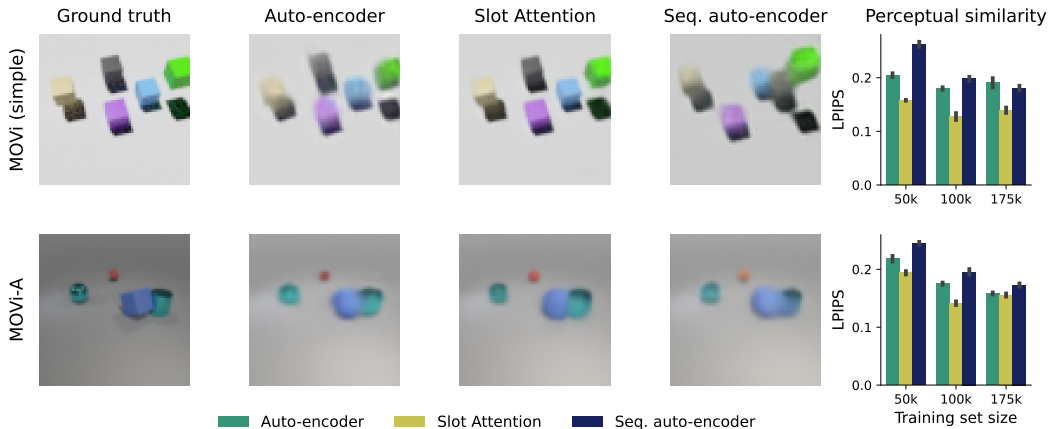


Figure 5: Reconstructions and LPIPS similarity for different models on the MOVi (simple) and MOVi-A datasets. Auto-encoding models without object slots approach or match the reconstruction ability of Slot Attention on novel object configurations in the MOVi domain.

5 THE BENEFITS OF PARTIALLY ENTANGLED REPRESENTATIONS

Even though unsupervised training on images of objects leads to linearly decodable representations of objects, especially in the dynamic model class, the representations of objects do not ever become completely disjoint (see Figure 6). That is, the models rely on distributed codes in their latent spaces that often represent distinct objects using overlapping populations of neurons. Yet this does not seem to impact the models’ ability to perform compositional generalization, e.g. predict dynamics and reconstruct scenes of novel compositions of objects.

To get a better qualitative understanding for the degree of object separability, we analysed the trained CWM’s and their slotted counterparts’ representations and the degree to which they showed systematic similarities. We obtained object representations of 300 initial frames x_t and successor frames x_{t+1} where only one object changed in one aspect from t to $t + 1$ in the cubes and Multi-dSprites domains. We chose these domains since they had actions that accompanied the dynamics. Earlier, we used the absolute difference between these representations $|\Delta|$ to get a sense of how objects were represented. However, one could also use these absolute differences to get a sense of how *transformations* or *actions* that acted on objects were represented. For instance, pushing the red cube along the y -axis on the grid might cause a similar change in representation as pushing the blue cube along the y -axis, even though the same action is applied to different objects. Analogously, in the Multi-dSprites domain, shrinking or rotating the heart sprite could induce similar representational changes as shrinking and rotating the square sprite. We do not expect to see this for slotted models, as they are more likely to represent the properties of different objects in orthogonal sub-spaces.

For both model types and datasets we obtained the absolute representational change $|\Delta|$ for all 300 frame pairs and computed pairwise similarity matrices using cosine similarity as our metric (see Figure 6A). These matrices contained information about which *transitions* were represented similarly for both distributed and slotted models. First we sorted these similarity matrices according to *which object* changed. Here we see five clear object clusters for both models in the cubes domain, and four clusters in the Multi-dSprites domain, albeit to a lesser degree for the distributed models.

Next, we sorted the similarity matrices according to *which transformation or action* was applied to the objects. While action clusters are identifiable for the CSWM, intra-action similarities were significantly lower than for the CWM (see Figure 6B). Representing object properties in a shared representational space not only allows for systematic representations of objects, but can also give rise to systematic representations of *transformations* that act on objects.

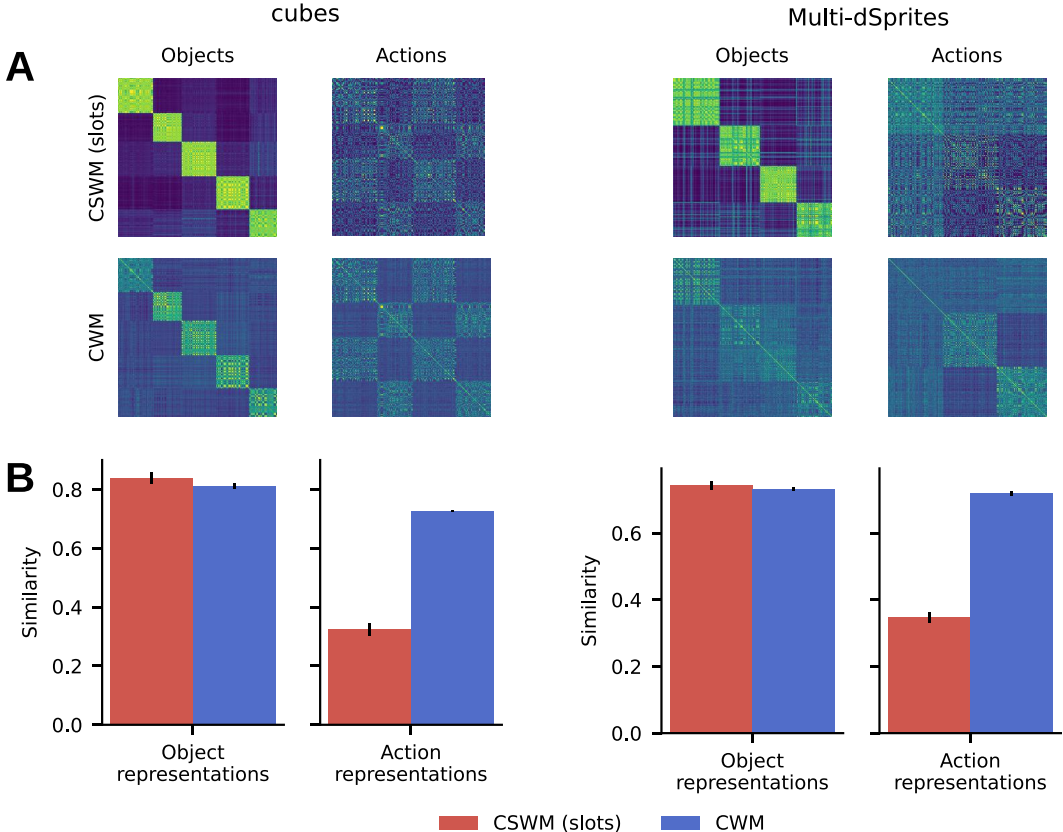


Figure 6: **A**: Representational similarity matrices showing cosine similarity of state transitions $|\Delta|$ for the CSWM and CWM on the cubes (left) and Multi-dSprites datasets (right). The cosine similarities are either ordered according to which object changed, or which action was performed on one the objects. In both cases, clusters are visible, though object clusters are more prominent in the slotted models, and action clusters more prominent in the distributed models. The cosine similarities are averaged over five seeds. **B**: CSWM intra-object similarity is significantly higher than its intra-action similarity, since object dynamics are isolated in separate subspaces. On the other hand, the CWM’s intra-action similarities are much closer to the intra-object similarities, allowing for richer generalization while preserving object separability.

5.1 DISTRIBUTED AND SLOTTED REPRESENTATIONAL ALIGNMENT INCREASES WITH MORE DATA

It has recently been argued that deep neural network models’ representations tend to grow more and more similar as training data size and model sizes increase (Huh et al., 2024). Do we see a similar convergence in latent representations of scenes composed of objects?

We extracted representations from all five seeds and all dataset sizes for CWM and the Auto-encoding models in the cubes, 3-body physics and Multi-dSprites domains, and compared them to the corresponding representations of the object-centric CSWM models. Next we computed the Euclidean distance between all pairs of representations for all models in the three different domains, and then calculated the degree of correlation between these distance matrices of the different models. If two models’ distance matrices were highly positively correlated, they perceived the same pairs of images as similar and dissimilar. In other words, their representations show a high degree of *alignment*.

In all three domains we see that the CWM’s representations grow more and more aligned to those of the CSWM with more data, reaching a score of around 0.8 on average in the largest data setting (see Figure 7). This indicates that, while alignment can increase substantially with enough data, simple

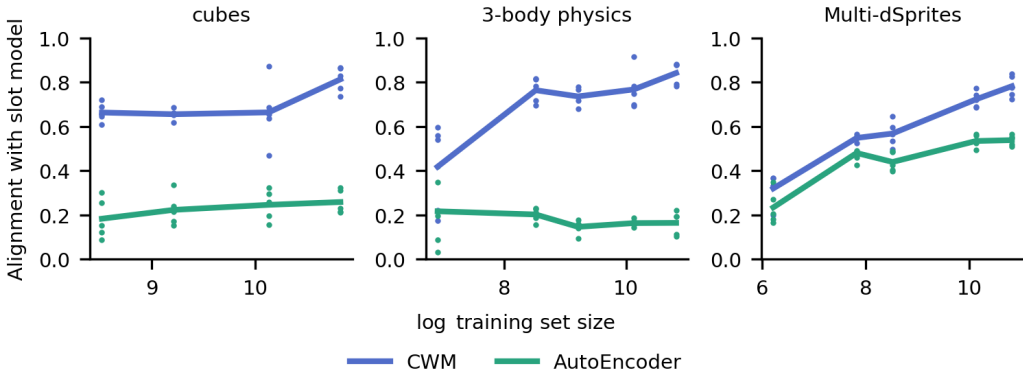


Figure 7: Alignment with slot models as determined by representational similarity alignment (RSA) (Kriegeskorte et al., 2008; Kornblith et al., 2019). The representations of the contrastive model (CWM) become more aligned with its’ slotted counterpart with more data.

architectural features can leave gaps, as for instance shown in Section 5. We did not observe this trend with the auto-encoder, which showed a significantly lower level of alignment with the CSWM. This suggests that, while data can drive alignment, this has to be paired with an appropriate loss function.

6 DISCUSSION

6.1 LIMITATIONS

Our study has focused on unsupervised representation learning models, paired with static and dynamic prediction objectives. However, the space of unsupervised learning techniques is vast. Future work should investigate object-separability in *self-supervised* representation learning settings (Grill et al., 2020; Zbontar et al., 2021; Schwarzer et al., 2020). Moreover, other model architectures like Vision Transformers (Dosovitskiy et al., 2020) are promising, as their attention patterns have been shown to match segmentation masks of natural images of objects (Caron et al., 2021).

The degree to which these properties scale to naturalistic and real-world video datasets is unclear. A natural next step is to compare larger slotted architectures, such as VideoSAUR (Zadaianchuk et al., 2024), to distributed models on naturalistic videos. It is possible that in these complex, real world domains, relying on richer, more entangled representations can facilitate generalization. Lastly, regularization and information bottleneck methods may significantly aid in learning separable object representations as well (Alemi et al., 2016; Shamir et al., 2010).

6.2 CONCLUSION

We have shown that models without object slots can learn object representations that are disentangled enough to be *separable*, but entangled enough to support generalization about *transformations* of objects. Furthermore, training models to predict object dynamics significantly improved object separability. We believe our findings are important because they highlight multiple ways in which a representation can be beneficial for generalization: Slotted models can seamlessly decompose the world into its constituent objects, facilitating compositional generalization. Models with simpler, unconstrained latent spaces can decompose the world in ways that also separate objects, while allowing information about one object’s dynamics and properties to permeate to others.

ACKNOWLEDGEMENTS

We thank the HCAI lab for valuable feedback and comments throughout the project. This work was supported by the Institute for Human-Centered AI at the Helmholtz Center for Computational Health, the Volkswagen Foundation, the Max Planck Society, the German Federal Ministry of Education and Research (BMBF): Tübingen AI Center, FKZ: 01IS18039A, and funded by the Deutsche Forschungsgemeinschaft (DFG, German Research Foundation) under Germany’s Excellence Strategy–EXC2064/1–390727645.15/18.

REFERENCES

- Alexander A Alemi, Ian Fischer, Joshua V Dillon, and Kevin Murphy. Deep variational information bottleneck. *arXiv preprint arXiv:1612.00410*, 2016.
- Yoshua Bengio, Aaron Courville, and Pascal Vincent. Representation learning: A review and new perspectives. *IEEE transactions on pattern analysis and machine intelligence*, 35(8):1798–1828, 2013.
- Jack Brady, Roland S Zimmermann, Yash Sharma, Bernhard Schölkopf, Julius von Kügelgen, and Wieland Brendel. Provably learning object-centric representations. *arXiv preprint arXiv:2305.14229*, 2023.
- Christopher P Burgess, Irina Higgins, Arka Pal, Loic Matthey, Nick Watters, Guillaume Desjardins, and Alexander Lerchner. Understanding disentangling in *beta*-vae. *arXiv preprint arXiv:1804.03599*, 2018.
- Mathilde Caron, Hugo Touvron, Ishan Misra, Hervé Jégou, Julien Mairal, Piotr Bojanowski, and Armand Joulin. Emerging properties in self-supervised vision transformers. In *Proceedings of the IEEE/CVF international conference on computer vision*, pp. 9650–9660, 2021.
- Ting Chen, Simon Kornblith, Mohammad Norouzi, and Geoffrey Hinton. A simple framework for contrastive learning of visual representations. In *International conference on machine learning*, pp. 1597–1607. PMLR, 2020.
- Can Demircan, Tankred Saanum, Leonardo Pettini, Marcel Binz, Blazej M Baczkowski, Paula Kaanders, Christian F Doeller, Mona M Garvert, and Eric Schulz. Language aligned visual representations predict human behavior in naturalistic learning tasks. *arXiv preprint arXiv:2306.09377*, 2023.
- Andrea Dittadi, Samuele Papa, Michele De Vita, Bernhard Schölkopf, Ole Winther, and Francesco Locatello. Generalization and robustness implications in object-centric learning. *arXiv preprint arXiv:2107.00637*, 2021.
- Alexey Dosovitskiy, Lucas Beyer, Alexander Kolesnikov, Dirk Weissenborn, Xiaohua Zhai, Thomas Unterthiner, Mostafa Dehghani, Matthias Minderer, Georg Heigold, Sylvain Gelly, et al. An image is worth 16x16 words: Transformers for image recognition at scale. In *International Conference on Learning Representations*, 2020.
- Gamaleldin Elsayed, Aravindh Mahendran, Sjoerd van Steenkiste, Klaus Greff, Michael C Mozer, and Thomas Kipf. Savi++: Towards end-to-end object-centric learning from real-world videos. *Advances in Neural Information Processing Systems*, 35:28940–28954, 2022.
- Mona M Garvert, Tankred Saanum, Eric Schulz, Nicolas W Schuck, and Christian F Doeller. Hippocampal spatio-predictive cognitive maps adaptively guide reward generalization. *Nature Neuroscience*, 26(4):615–626, 2023.
- Carles Gelada, Saurabh Kumar, Jacob Buckman, Ofir Nachum, and Marc G Bellemare. Deepmdp: Learning continuous latent space models for representation learning. In *International conference on machine learning*, pp. 2170–2179. PMLR, 2019.
- Noah D Goodman, Joshua B Tenenbaum, Jacob Feldman, and Thomas L Griffiths. A rational analysis of rule-based concept learning. *Cognitive science*, 32(1):108–154, 2008.

- Klaus Greff, Raphaël Lopez Kaufman, Rishabh Kabra, Nick Watters, Christopher Burgess, Daniel Zoran, Loic Matthey, Matthew Botvinick, and Alexander Lerchner. Multi-object representation learning with iterative variational inference. In *International Conference on Machine Learning*, pp. 2424–2433. PMLR, 2019.
- Klaus Greff, Sjoerd Van Steenkiste, and Jürgen Schmidhuber. On the binding problem in artificial neural networks. *arXiv preprint arXiv:2012.05208*, 2020.
- Klaus Greff, Francois Belletti, Lucas Beyer, Carl Doersch, Yilun Du, Daniel Duckworth, David J Fleet, Dan Gnanapragasam, Florian Golemo, Charles Herrmann, Thomas Kipf, Abhijit Kundu, Dmitry Lagun, Issam Laradji, Hsueh-Ti (Derek) Liu, Henning Meyer, Yishu Miao, Derek Nowrouzezahrai, Cengiz Oztireli, Etienne Pot, Noha Radwan, Daniel Rebain, Sara Sabour, Mehdi S. M. Sajjadi, Matan Sela, Vincent Sitzmann, Austin Stone, Deqing Sun, Suhani Vora, Ziyu Wang, Tianhao Wu, Kwang Moo Yi, Fangcheng Zhong, and Andrea Tagliasacchi. Kubric: a scalable dataset generator. 2022.
- Jean-Bastien Grill, Florian Strub, Florent Alché, Corentin Tallec, Pierre Richemond, Elena Buchatskaya, Carl Doersch, Bernardo Avila Pires, Zhaohan Guo, Mohammad Gheshlaghi Azar, et al. Bootstrap your own latent—a new approach to self-supervised learning. *Advances in neural information processing systems*, 33:21271–21284, 2020.
- Kaiming He, Xinlei Chen, Saining Xie, Yanghao Li, Piotr Dollár, and Ross Girshick. Masked auto-encoders are scalable vision learners. In *Proceedings of the IEEE/CVF conference on computer vision and pattern recognition*, pp. 16000–16009, 2022.
- Irina Higgins, Loic Matthey, Arka Pal, Christopher Burgess, Xavier Glorot, Matthew Botvinick, Shakir Mohamed, and Alexander Lerchner. beta-vae: Learning basic visual concepts with a constrained variational framework. In *International conference on learning representations*, 2016.
- Irina Higgins, Nicolas Sonnerat, Loic Matthey, Arka Pal, Christopher P Burgess, Matko Bosnjak, Murray Shanahan, Matthew Botvinick, Demis Hassabis, and Alexander Lerchner. Scan: Learning hierarchical compositional visual concepts. *arXiv preprint arXiv:1707.03389*, 2017.
- Irina Higgins, David Amos, David Pfau, Sebastien Racaniere, Loic Matthey, Danilo Rezende, and Alexander Lerchner. Towards a definition of disentangled representations. *arXiv preprint arXiv:1812.02230*, 2018.
- Minyoung Huh, Brian Cheung, Tongzhou Wang, and Phillip Isola. The platonic representation hypothesis. *arXiv preprint arXiv:2405.07987*, 2024.
- Hyunjik Kim and Andriy Mnih. Disentangling by factorising. In *International Conference on Machine Learning*, pp. 2649–2658. PMLR, 2018.
- Diederik P Kingma. Auto-encoding variational bayes. *arXiv preprint arXiv:1312.6114*, 2013.
- Diederik P Kingma and Jimmy Ba. Adam: A method for stochastic optimization. *arXiv preprint arXiv:1412.6980*, 2014.
- Thomas Kipf, Elise Van der Pol, and Max Welling. Contrastive learning of structured world models. *arXiv preprint arXiv:1911.12247*, 2019.
- Simon Kornblith, Mohammad Norouzi, Honglak Lee, and Geoffrey Hinton. Similarity of neural network representations revisited. In *International conference on machine learning*, pp. 3519–3529. PMLR, 2019.
- Nikolaus Kriegeskorte, Marieke Mur, and Peter A Bandettini. Representational similarity analysis—connecting the branches of systems neuroscience. *Frontiers in systems neuroscience*, 2:249, 2008.
- Brenden M Lake, Ruslan Salakhutdinov, and Joshua B Tenenbaum. Human-level concept learning through probabilistic program induction. *Science*, 350(6266):1332–1338, 2015.
- Brenden M Lake, Tomer D Ullman, Joshua B Tenenbaum, and Samuel J Gershman. Building machines that learn and think like people. *Behavioral and brain sciences*, 40:e253, 2017.

- Michael Laskin, Aravind Srinivas, and Pieter Abbeel. Curl: Contrastive unsupervised representations for reinforcement learning. In *International conference on machine learning*, pp. 5639–5650. PMLR, 2020.
- Francesco Locatello, Stefan Bauer, Mario Lucic, Gunnar Raetsch, Sylvain Gelly, Bernhard Schölkopf, and Olivier Bachem. Challenging common assumptions in the unsupervised learning of disentangled representations. In *international conference on machine learning*, pp. 4114–4124. PMLR, 2019.
- Francesco Locatello, Stefan Bauer, Mario Lucic, Gunnar Rätsch, Sylvain Gelly, Bernhard Schölkopf, and Olivier Bachem. A sober look at the unsupervised learning of disentangled representations and their evaluation. *The Journal of Machine Learning Research*, 21(1):8629–8690, 2020a.
- Francesco Locatello, Dirk Weissenborn, Thomas Unterthiner, Aravindh Mahendran, Georg Heigold, Jakob Uszkoreit, Alexey Dosovitskiy, and Thomas Kipf. Object-centric learning with slot attention. *Advances in Neural Information Processing Systems*, 33:11525–11538, 2020b.
- Christopher G Lucas, Thomas L Griffiths, Joseph J Williams, and Michael L Kalish. A rational model of function learning. *Psychonomic bulletin & review*, 22(5):1193–1215, 2015.
- Loic Matthey, Irina Higgins, Demis Hassabis, and Alexander Lerchner. dsprites: Disentanglement testing sprites dataset, 2017.
- Vinod Nair and Geoffrey E Hinton. Rectified linear units improve restricted boltzmann machines. In *Icml*, 2010.
- Alec Radford, Jeffrey Wu, Rewon Child, David Luan, Dario Amodei, Ilya Sutskever, et al. Language models are unsupervised multitask learners. *OpenAI blog*, 1(8):9, 2019.
- Alec Radford, Jong Wook Kim, Chris Hallacy, Aditya Ramesh, Gabriel Goh, Sandhini Agarwal, Girish Sastry, Amanda Askell, Pamela Mishkin, Jack Clark, et al. Learning transferable visual models from natural language supervision. In *International conference on machine learning*, pp. 8748–8763. PMLR, 2021.
- Karl Ridgeway and Michael C Mozer. Learning deep disentangled embeddings with the f-statistic loss. *Advances in neural information processing systems*, 31, 2018.
- Tankred Saanum, Peter Dayan, and Eric Schulz. Predicting the future with simple world models. *arXiv preprint arXiv:2401.17835*, 2024.
- Luca M Schulze Buschhoff, Eric Schulz, and Marcel Binz. The acquisition of physical knowledge in generative neural networks. In *Proceedings of the 40th international conference on machine learning*, pp. 30321–30341, 2023.
- Max Schwarzer, Ankesh Anand, Rishab Goel, R Devon Hjelm, Aaron Courville, and Philip Bachman. Data-efficient reinforcement learning with self-predictive representations. *arXiv preprint arXiv:2007.05929*, 2020.
- Maximilian Seitzer, Max Horn, Andrii Zadaianchuk, Dominik Zietlow, Tianjun Xiao, Carl-Johann Simon-Gabriel, Tong He, Zheng Zhang, Bernhard Schölkopf, Thomas Brox, et al. Bridging the gap to real-world object-centric learning. *arXiv preprint arXiv:2209.14860*, 2022.
- Ohad Shamir, Sivan Sabato, and Naftali Tishby. Learning and generalization with the information bottleneck. *Theoretical Computer Science*, 411(29-30):2696–2711, 2010.
- Alex J Smola and Bernhard Schölkopf. *Learning with kernels*, volume 4. Citeseer, 1998.
- Joshua B Tenenbaum, Charles Kemp, Thomas L Griffiths, and Noah D Goodman. How to grow a mind: Statistics, structure, and abstraction. *science*, 331(6022):1279–1285, 2011.
- Thaddäus Wiedemer, Jack Brady, Alexander Panfilov, Attila Juhos, Matthias Bethge, and Wieland Brendel. Provable compositional generalization for object-centric learning. *arXiv preprint arXiv:2310.05327*, 2023.

- Ziyi Wu, Nikita Dvornik, Klaus Greff, Thomas Kipf, and Animesh Garg. Slotformer: Unsupervised visual dynamics simulation with object-centric models. *arXiv preprint arXiv:2210.05861*, 2022.
- Denis Yarats, Rob Fergus, Alessandro Lazaric, and Lerrel Pinto. Mastering visual continuous control: Improved data-augmented reinforcement learning. *arXiv preprint arXiv:2107.09645*, 2021a.
- Denis Yarats, Amy Zhang, Ilya Kostrikov, Brandon Amos, Joelle Pineau, and Rob Fergus. Improving sample efficiency in model-free reinforcement learning from images. In *Proceedings of the aaai conference on artificial intelligence*, volume 35, pp. 10674–10681, 2021b.
- Andrii Zadaianchuk, Maximilian Seitzer, and Georg Martius. Object-centric learning for real-world videos by predicting temporal feature similarities. *Advances in Neural Information Processing Systems*, 36, 2024.
- Jure Zbontar, Li Jing, Ishan Misra, Yann LeCun, and Stéphane Deny. Barlow twins: Self-supervised learning via redundancy reduction. In *International conference on machine learning*, pp. 12310–12320. PMLR, 2021.
- Richard Zhang, Phillip Isola, Alexei A Efros, Eli Shechtman, and Oliver Wang. The unreasonable effectiveness of deep features as a perceptual metric. In *Proceedings of the IEEE conference on computer vision and pattern recognition*, pp. 586–595, 2018.

A APPENDIX

B ARCHITECTURE AND HYPERPARAMETERS

B.1 CONVOLUTIONAL NEURAL NETWORKS

For our image encoders we rely on a standard CNN architecture used in other works such as Yarats et al. (2021b;a). For the 3-body physics dataset we stacked two frames, as in Kipf et al. (2019) to provide information about directional velocity.

```
import torch
from torch import nn
encoder = nn.Sequential(
    nn.Conv2d(num_channels, 32, 3, stride=2),
    nn.ReLU(),

    nn.Conv2d(32, 32, 3, stride=1),
    nn.ReLU(),

    nn.Conv2d(32, 32, 3, stride=1),
    nn.ReLU(),

    nn.Conv2d(32, 32, 3, stride=1),
    nn.ReLU()
)
```

This network is followed by an MLP with 2 hidden layers and 512 hidden units. All models used ReLU (Nair & Hinton, 2010) activation functions and were optimized using Adam Kingma & Ba (2014). The CSWM and Slot Attention models were trained using the hyperparameters and encoder architectures provided in Kipf et al. (2019) and Locatello et al. (2020b), respectively.

B.2 TRANSFORMER

We use the causal Transformer architecture of GPT-2 (Radford et al., 2019), building on the implementation in the nanoGPT repository¹. In the slotted dynamics model, the transformer applied attention over the sequence of slots per time-step. Assuming K slots and T time-steps, the transformer applied attention over a sequence of $K \times T$ data-points. In MOVi (simple) we trained CSWM with 6 object slots, allowing each slot to model one object plus a background slot. In MOVi-A we trained CSWM with 11 object slots, allowing for 10 separate object representations plus the background. The Slot Attention model was trained with the same number of slots as CSWM. The transformers were trained with the following hyperparameters:

Table 1: Transformer hyperparameters.

| Hyperparameter | Value |
|--------------------|-------|
| MLP Hidden units | 2048 |
| Transformer blocks | 2 |
| Context length | 4 |
| Heads | 8 |

B.3 HYPERPARAMETERS

Below are specific hyperparameters for the different distributed model classes.

¹See <https://github.com/karpathy/nanoGPT>

Table 2: Contrastive model hyperparameters.

| Hyperparameter | Value |
|---------------------------|-------------------------|
| Hidden units | 512 |
| Batch size | 512 (1024 for MOVi) |
| MLP hidden layers | 2 |
| Latent dimensions $ z_t $ | 50 (500 for MOVi) |
| Margin λ | 1 (100 for MOVi) |
| Learning rate | 0.001 (0.0004 for MOVi) |

For auto-encoding models we use the transpose of the encoder networks presented above. These models are trained with the following hyperparameters:

Table 3: Auto-encoder hyperparameters.

| Hyperparameter | Value |
|---------------------------|-------------------------|
| Hidden units | 512 |
| Batch size | 512 (64 for MOVi) |
| MLP hidden layers | 2 |
| Latent dimensions $ z_t $ | 50 (500 for MOVi) |
| Learning rate | 0.001 (0.0004 for MOVi) |

Table 4: Sequential auto-encoder hyperparameters.

| Hyperparameter | Value |
|---------------------------|-------------------------|
| Hidden units | 512 |
| Batch size | 512 (124 for MOVi) |
| MLP hidden layers | 2 |
| Latent dimensions $ z_t $ | 50 (500 for MOVi) |
| Learning rate | 0.001 (0.0004 for MOVi) |

C OBJECT DECODABILITY BASELINE

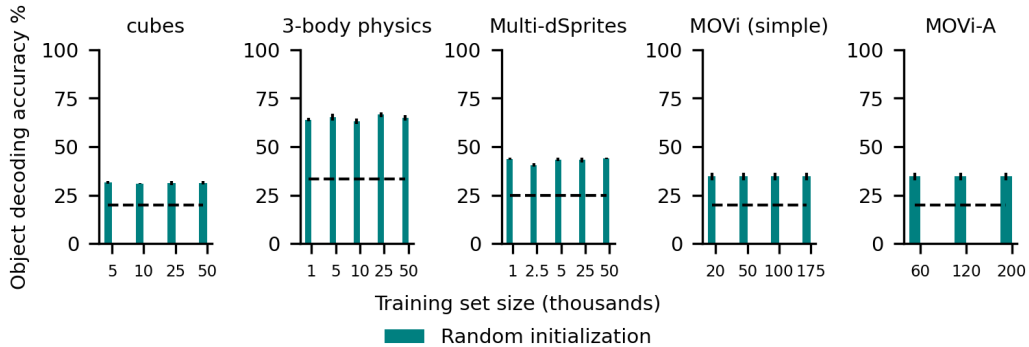


Figure 8: When initializing the image encoders randomly, the linear decodability of objects is higher than chance, but substantially lower than the level of trained models.

C.1 SLOTTED REPRESENTATIONS ARE RECOVERABLE FROM DISTRIBUTED REPRESENTATIONS

We assessed the degree to which CWMs representations could be mapped to discrete object slots in the `cubes` dataset. We trained a slot decoder network with the same architecture as the Slot Attention model to reconstruct images from the representations of CWM. Assuming K object slots, the decoder was trained to reconstruct the original frame as an additive composition of K individual objects. Crucially, we froze CWM’s encoder, meaning that the decoder could only use information learned through the contrastive dynamic training to re-compose the scene. We see that the slot decoder can not only learn to reconstruct the scenes with high fidelity, but also reconstruct the scenes by individually reconstructing the cubes and composing them.

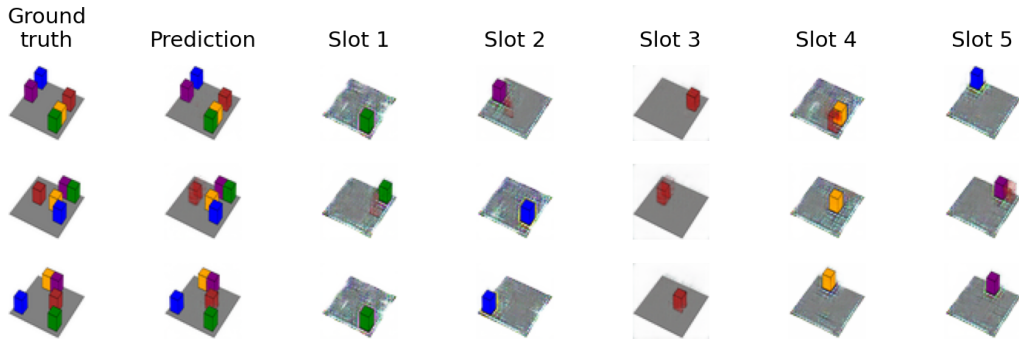


Figure 9: Training a slot-decoder to reconstruct scenes from CWM’s learned representations leads to scene re-compositions that track the original ground truth objects.